

TUM-HEP-455/02
 Alberta Thy 05-02
 IFT-5/2002
 hep-ph/0203135

Completing the NLO QCD calculation of $\bar{B} \rightarrow X_s \gamma$

Andrzej J. Buras¹, Andrzej Czarnecki², Mikołaj Misiak³ and Jörg Urban¹

¹*Physik Department, Technische Universität München,
 D-85748 Garching, Germany*

²*Department of Physics, University of Alberta,
 Edmonton, Alberta, Canada T6G 2J1*

³*Institute of Theoretical Physics, Warsaw University,
 Hoża 69, PL-00-681 Warsaw, Poland*

Abstract

We evaluate two-loop $b \rightarrow s \gamma$ matrix elements of all the four-quark operators containing no derivatives. Contrary to previous calculations, no expansion in the mass ratio m_c/m_b is performed, and all the possible Dirac and flavor structures are included. Consequently, we are able to provide the last item in the NLO analysis of $\bar{B} \rightarrow X_s \gamma$ that has been missing so far, namely the two-loop matrix elements of the QCD-penguin operators. Due to smallness of the Wilson coefficients of those operators in the Standard Model, their effect on the branching ratio is small: a reduction by roughly 1%. We find $\text{BR}[\bar{B} \rightarrow X_s \gamma]_{E_\gamma > 1.6 \text{ GeV}} = (3.57 \pm 0.30) \times 10^{-4}$.

1 Introduction

The decay $\bar{B} \rightarrow X_s \gamma$ constitutes a stringent test of the Standard Model (SM) and many of its extensions. In the theoretical prediction for its branching ratio, crucial role is played by the NLO QCD corrections to the $b \rightarrow s \gamma$ partonic amplitude. In the introduction to our previous article [1], status of the NLO calculations has been summarized. The only missing elements were two-loop matrix elements of the so-called QCD-penguin operators.

The present paper is devoted to evaluation of these matrix elements. Our results for two-loop diagrams are presented in such a manner that they can be applied to an arbitrary extension of the SM where additional four-quark operators arise, e.g. to the generic MSSM. Thus, apart from completing the NLO QCD calculation in the SM, we provide an important ingredient for analyses of new physics effects. Moreover, contrary to previous calculations [2, 1], no expansion in the mass ratio m_c/m_b is performed.

The article is organized as follows. In the next section, the relevant definitions are collected. In section 3, we summarize our results for the matrix elements, and describe consequences for $\text{BR}[\bar{B} \rightarrow X_s \gamma]$ in the SM. Section 4 contains details of the calculation for one set of the two-loop diagrams. For the remaining sets, we present only the final expressions in section 5. The renormalization procedure is described in section 6. Section 7 contains our conclusions.

2 The effective Hamiltonian

In the SM, the $b \rightarrow s \gamma$ transition is mediated by the effective Hamiltonian^{1,2}

$$\mathcal{H}_{\text{eff}} = -\frac{4G_F}{\sqrt{2}} V_{ts}^* V_{tb} \sum_{k=1}^8 C_k P_k, \quad (2.1)$$

where C_k are the Wilson coefficients and P_k stand for the following operators:

$$\begin{aligned} P_1 &= (\bar{s}_L \gamma_\mu T^a c_L)(\bar{c}_L \gamma^\mu T^a b_L), \\ P_2 &= (\bar{s}_L \gamma_\mu c_L)(\bar{c}_L \gamma^\mu b_L), \\ P_3 &= (\bar{s}_L \gamma_\mu b_L) \sum_q (\bar{q} \gamma^\mu q), \quad (q = u, d, s, c, b) \\ P_4 &= (\bar{s}_L \gamma_\mu T^a b_L) \sum_q (\bar{q} \gamma^\mu T^a q), \\ P_5 &= (\bar{s}_L \gamma_\mu \gamma_\nu \gamma_\rho b_L) \sum_q (\bar{q} \gamma^\mu \gamma^\nu \gamma^\rho q), \end{aligned}$$

¹ It is written in terms of bare quantities here. The renormalized interaction terms can be found in eq. (6.1).

²For simplicity, we set V_{ub} to zero in all our formulae. However, its non-zero value will be included in the phenomenological analysis, as in eq. (3.7) of ref. [3].

$$\begin{aligned}
P_6 &= (\bar{s}_L \gamma_\mu \gamma_\nu \gamma_\rho T^a b_L) \sum_q (\bar{q} \gamma^\mu \gamma^\nu \gamma^\rho T^a q), \\
P_7 &= \frac{e}{16\pi^2} m_b (\bar{s}_L \sigma^{\mu\nu} b_R) F_{\mu\nu}, \\
P_8 &= \frac{g}{16\pi^2} m_b (\bar{s}_L \sigma^{\mu\nu} T^a b_R) G_{\mu\nu}^a.
\end{aligned} \tag{2.2}$$

In order to match our computation with the NLO results for C_k , we adopt here the same operator basis as in ref. [4].

Instead of the original Wilson coefficients C_k it is convenient to use certain linear combinations of them, the so-called “effective coefficients” [5]

$$C_k^{\text{eff}} = \begin{cases} C_k, & \text{for } k = 1, \dots, 6, \\ C_7 + \sum_{i=1}^6 y_i C_i, & \text{for } k = 7, \\ C_8 + \sum_{i=1}^6 z_i C_i, & \text{for } k = 8. \end{cases} \tag{2.3}$$

The numbers y_i and z_i are defined so that the leading-order $b \rightarrow s\gamma$ and $b \rightarrow s$ *gluon* matrix elements of the effective Hamiltonian are proportional to the leading-order terms in C_7^{eff} and C_8^{eff} , respectively. In the NDR scheme,

$$\vec{y} = \left(0, 0, -\frac{1}{3}, -\frac{4}{9}, -\frac{20}{3}, -\frac{80}{9}\right), \quad \vec{z} = \left(0, 0, 1, -\frac{1}{6}, 20, -\frac{10}{3}\right). \tag{2.4}$$

The renormalization group equations for the $\overline{\text{MS}}$ -renormalized effective coefficients read

$$\mu \frac{d}{d\mu} C_i^{\text{eff}}(\mu) = C_j^{\text{eff}}(\mu) \gamma_{ji}^{\text{eff}}(\mu). \tag{2.5}$$

Explicit results for the coefficients

$$C_i^{\text{eff}}(\mu) = C_i^{(0)\text{eff}}(\mu) + \frac{\alpha_s(\mu)}{4\pi} C_i^{(1)\text{eff}}(\mu) + \mathcal{O}(\alpha_s^2) \tag{2.6}$$

and the matrix

$$\hat{\gamma}^{\text{eff}} = \frac{\alpha_s}{4\pi} \hat{\gamma}^{(0)\text{eff}} + \left(\frac{\alpha_s}{4\pi}\right)^2 \hat{\gamma}^{(1)\text{eff}} + \mathcal{O}(\alpha_s^3) \tag{2.7}$$

can be found in ref. [4] (see also eq. (6.3) here). The partonic decay rate from eqs. (29)–(32) of that article can be expressed as follows:

$$\Gamma[b \rightarrow X_s \gamma]^{E_\gamma > E_0} = \frac{G_F^2 \alpha_{em} m_b^5}{32\pi^4} |V_{ts}^* V_{tb}|^2 \left[|D|^2 + A + \mathcal{O}(\alpha_s^2, \alpha_{em}) \right], \tag{2.8}$$

where, for $\mu \sim m_b$,

$$D = \left(\text{Terms proportional to } C_7^{\text{eff}}(\mu) \right) + \frac{\alpha_s}{4\pi} \sum_{\substack{1 \leq k \leq 8 \\ k \neq 7}} C_k^{(0)\text{eff}}(\mu) \left[r_k + \gamma_{k7}^{(0)\text{eff}} \ln \frac{m_b}{\mu} \right], \tag{2.9}$$

$$A = \left(\text{Terms proportional to } |C_7^{(0)\text{eff}}(\mu)|^2 \right) + \left(\text{Terms vanishing when } E_0 \rightarrow \frac{m_b}{2} \right). \tag{2.10}$$

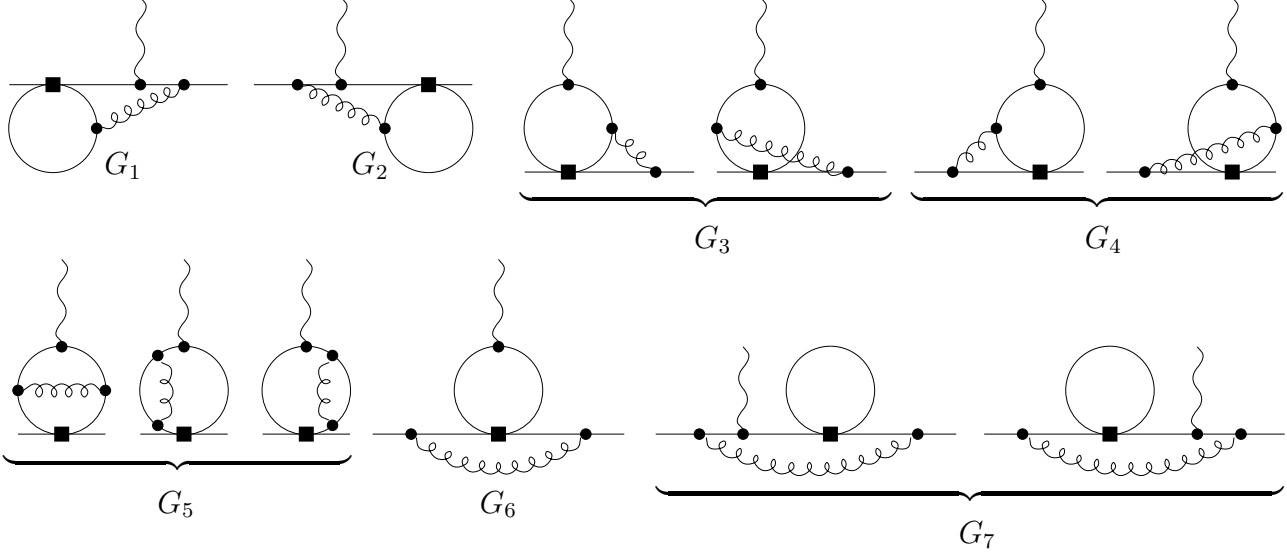


Figure 1: Two-loop 1PI contributions to the matrix elements of P_k .

For $k = 1, \dots, 6$, the quantities r_k in eq. (2.9) can be found by calculating the two-loop $b \rightarrow s\gamma$ matrix elements of the four-quark operators P_k . The relevant Feynman diagrams are presented in fig. 1, where the square boxes denote the operator insertions. On the other hand, r_8 is given by the one-loop matrix element of P_8 .

3 Final results for r_k and consequences for $\text{BR}[\bar{B} \rightarrow X_s \gamma]$

Calculation of r_k in eq. (2.9) has been the main goal of the present paper. For $k = 1, 2, 8$, we confirm the findings of refs. [2, 1]. For $k = 3, \dots, 6$, our results are new. Altogether, they read

$$\begin{aligned}
r_1 &= \frac{833}{729} - \frac{1}{3}[a(z) + b(z)] + \frac{40}{243}i\pi, \\
r_2 &= -\frac{1666}{243} + 2[a(z) + b(z)] - \frac{80}{81}i\pi, \\
r_3 &= \frac{2392}{243} + \frac{8\pi}{3\sqrt{3}} + \frac{32}{9}X_b - a(1) + 2b(1) + \frac{56}{81}i\pi, \\
r_4 &= -\frac{761}{729} - \frac{4\pi}{9\sqrt{3}} - \frac{16}{27}X_b + \frac{1}{6}a(1) + \frac{5}{3}b(1) + 2b(z) - \frac{148}{243}i\pi, \\
r_5 &= \frac{56680}{243} + \frac{32\pi}{3\sqrt{3}} + \frac{128}{9}X_b - 16a(1) + 32b(1) + \frac{896}{81}i\pi, \\
r_6 &= \frac{5710}{729} - \frac{16\pi}{9\sqrt{3}} - \frac{64}{27}X_b - \frac{10}{3}a(1) + \frac{44}{3}b(1) + 12a(z) + 20b(z) - \frac{2296}{243}i\pi, \\
r_8 &= \frac{44}{9} - \frac{8}{27}\pi^2 + \frac{8}{9}i\pi,
\end{aligned} \tag{3.1}$$

where $z = m_c^2/m_b^2$. Similar ratios for the light quarks (u, d, s) have been set to zero. The constant X_b is given by

$$X_b = \int_0^1 dx \int_0^1 dy \int_0^1 dv \, xy \ln[v + x(1-x)(1-v)(1-v+vy)] \simeq -0.1684. \tag{3.2}$$

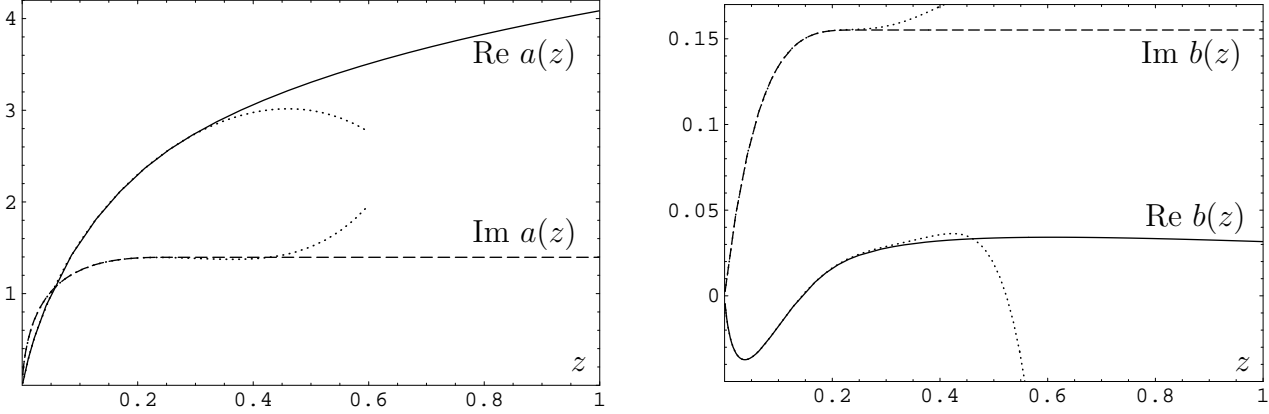


Figure 2: Functions $a(z)$ and $b(z)$. Dotted lines represent their expansions at $z = 0$ up to $\mathcal{O}(z^6)$.

Exact expressions for the functions $a(z)$ and $b(z)$ are as follows:

$$a(z) = \frac{8}{9} \int_0^1 dx \int_0^1 dy \int_0^1 dv \{ [2 - v + xy(2v - 3)] \ln[vz + x(1 - x)(1 - v)(1 - v + vy)] \\ + [1 - v + xy(2v - 1)] \ln[z - i\varepsilon - x(1 - x)yv] \} + \frac{43}{9} + \frac{4}{9}i\pi, \quad (3.3)$$

$$b(z) = \frac{4}{81} \ln z + \frac{16}{27} z^2 + \frac{224}{81} z - \frac{92}{243} + \frac{4}{81} i\pi + \frac{-48z^2 - 64z + 4}{81} \sqrt{1 - 4z} f(z) - \frac{8}{9} z^2 \left(\frac{2}{3} z - 1 \right) f(z)^2 \\ - \frac{8}{9} \int_0^1 dx \int_0^1 dy \frac{\frac{1}{2} y^2 (y^2 - 1) x(1 - x) + (2 - y) u_1 \ln u_1 + (2y^2 - 2y - 1) u_2 \ln u_2}{(1 - y)^2}, \quad (3.4)$$

with $u_k = y^k x(1 - x) + (1 - y)z$, $\sqrt{-1} = +i$ and

$$f(z) = \theta(1 - 4z) \left(\ln \frac{1 + \sqrt{1 - 4z}}{1 - \sqrt{1 - 4z}} - i\pi \right) - 2i\theta(4z - 1) \arctan \frac{1}{\sqrt{4z - 1}}. \quad (3.5)$$

Additive constants in the functions a and b have been chosen in such a manner that $a(0) = b(0) = 0$. Our results for $a(1)$ and $b(1)$ read

$$a(1) \simeq 4.0859 + \frac{4}{9}i\pi, \quad (3.6)$$

$$b(1) = \frac{320}{81} - \frac{4\pi}{3\sqrt{3}} + \frac{632}{1215}\pi^2 - \frac{8}{45} \left[\frac{d^2 \ln \Gamma(x)}{dx^2} \right]_{x=\frac{1}{6}} + \frac{4}{81}i\pi \simeq 0.0316 + \frac{4}{81}i\pi. \quad (3.7)$$

There is no need to apply numerical integration for $z = m_c^2/m_b^2 \sim 0.1$, because, as illustrated in fig. 2, both functions are then accurately given by their expansions in z [2, 1],

$$a(z) = \frac{16}{9} \left\{ \left[\frac{5}{2} - \frac{1}{3}\pi^2 - 3\zeta(3) + \left(\frac{5}{2} - \frac{3}{4}\pi^2 \right) L + \frac{1}{4}L^2 + \frac{1}{12}L^3 \right] z \right. \\ + \left[\frac{7}{4} + \frac{2}{3}\pi^2 - \frac{1}{2}\pi^2 L - \frac{1}{4}L^2 + \frac{1}{12}L^3 \right] z^2 + \left[-\frac{7}{6} - \frac{1}{4}\pi^2 + 2L - \frac{3}{4}L^2 \right] z^3 \\ + \left[\frac{457}{216} - \frac{5}{18}\pi^2 - \frac{1}{72}L - \frac{5}{6}L^2 \right] z^4 + \left[\frac{35101}{8640} - \frac{35}{72}\pi^2 - \frac{185}{144}L - \frac{35}{24}L^2 \right] z^5 \\ + \left[\frac{67801}{8000} - \frac{21}{20}\pi^2 - \frac{3303}{800}L - \frac{63}{20}L^2 \right] z^6 + i\pi \left[\left(2 - \frac{1}{6}\pi^2 + \frac{1}{2}L + \frac{1}{2}L^2 \right) z \right. \\ \left. + \left(\frac{1}{2} - \frac{1}{6}\pi^2 - L + \frac{1}{2}L^2 \right) z^2 + z^3 + \frac{5}{9}z^4 + \frac{49}{72}z^5 + \frac{231}{200}z^6 \right] \} + \mathcal{O}(z^7 L^2), \quad (3.8)$$

$$\begin{aligned}
b(z) = & -\frac{8}{9} \left\{ \left(-3 + \frac{1}{6}\pi^2 - L \right) z - \frac{2}{3}\pi^2 z^{3/2} + \left(\frac{1}{2} + \pi^2 - 2L - \frac{1}{2}L^2 \right) z^2 \right. \\
& + \left(-\frac{25}{12} - \frac{1}{9}\pi^2 - \frac{19}{18}L + 2L^2 \right) z^3 + \left[-\frac{1376}{225} + \frac{137}{30}L + 2L^2 + \frac{2}{3}\pi^2 \right] z^4 \\
& + \left[-\frac{131317}{11760} + \frac{887}{84}L + 5L^2 + \frac{5}{3}\pi^2 \right] z^5 + \left[-\frac{2807617}{97200} + \frac{16597}{540}L + 14L^2 + \frac{14}{3}\pi^2 \right] z^6 \\
& \left. + i\pi \left[-z + (1 - 2L)z^2 + \left(-\frac{10}{9} + \frac{4}{3}L \right) z^3 + z^4 + \frac{2}{3}z^5 + \frac{7}{9}z^6 \right] \right\} + \mathcal{O}(z^7 L^2), \quad (3.9)
\end{aligned}$$

where $L = \ln z$.

	$\frac{m_c}{m_b} = 0.22$		$\frac{m_c}{m_b} = 0.29$	
	Re r_i	Im r_i	Re r_i	Im r_i
r_1	0.8309	0.1498	0.6821	0.0750
r_2	-4.9854	-0.8988	-4.0929	-0.4499
r_3	10.0589	1.0860	10.0589	1.0860
r_4	-1.0890	-1.2409	-1.0655	-1.1732
r_5	185.8412	17.3757	185.8412	17.3757
r_6	2.7855	-18.1132	8.2345	-15.1493
r_8	1.9646	2.7925	1.9646	2.7925

Table 1: Real and imaginary parts of r_k for two different values of m_c/m_b .

The numerical values of r_k for two different values of m_c/m_b are presented in table 1. We observe that the real parts of r_3 and r_5 are considerably larger than the remaining ones. If r_4 were as large as r_3 , its effect on the SM branching ratio would be around 6%. On the other hand, the size of r_5 is somewhat artificial — it is due in part to the lack of a “natural” factor $\frac{1}{16}$ in the definition of P_5 (2.2).

In order to calculate $\text{BR}[\bar{B} \rightarrow X_s \gamma]$, we use the NLO formulae collected in ref. [3]. The only elements that must be modified due to non-zero values of r_3, \dots, r_6 are the so-called “magic numbers”. Their updated values are presented in table 2. Once they are used, and the same computer program with the same numerical inputs is applied,³ we find

$$\text{BR}[\bar{B} \rightarrow X_s \gamma]_{E_\gamma > 1.6 \text{ GeV}}^{\text{subtracted } \psi, \psi'} = (3.57 \pm 0.30) \times 10^{-4}, \quad (3.10)$$

which is only a little lower than $(3.60 \pm 0.30) \times 10^{-4}$ in eq. (4.14) of ref. [3]. For the cutoff energy of $\frac{1}{20}m_b$ (which corresponds to the fake “total rate”), the effect on the branching ratio

³ One exception is ε_{ew} from eq. (4.6) of ref. [3] which we change to 0.0071 according to ref. [6]. This modification slightly diminishes the net effect on the branching ratio.

k	1	2	3	4	5	6	7	8
a_k	$\frac{14}{23}$	$\frac{16}{23}$	$\frac{6}{23}$	$-\frac{12}{23}$	0.4086	-0.4230	-0.8994	0.1456
d_k	1.4107	-0.8380	-0.4286	-0.0714	-0.6494	-0.0380	-0.0185	-0.0057
\tilde{d}_k	-17.6507	11.3460	2.4692	-0.8056	4.8898	-0.2308	-0.5290	0.1994
\tilde{d}_k^η	9.2746	-6.9366	-0.8740	0.4218	-2.7231	0.4083	0.1465	0.0205
\tilde{d}_k^a	0	0	0.8571	0.6667	0.1298	0.1951	0.1236	0.0276
\tilde{d}_k^b	0	0	0.8571	0.6667	0.2637	0.2906	-0.0611	-0.0171
$\tilde{d}_k^{i\pi}$	0.4702	0	-0.4268	-0.2222	-0.9042	-0.1150	-0.0975	0.0115
e_k	5.2620	-3.8412	0	0	-1.9043	-0.1008	0.1216	0.0183

Table 2: Update of table 1 from ref. [3]. Only \tilde{d}_k , \tilde{d}_k^a , \tilde{d}_k^b , $\tilde{d}_k^{i\pi}$ for $k = 3, \dots, 8$ are affected.

is the same: the central value decreases from 3.73×10^{-4} to 3.70×10^{-4} .

Such a small effect of the non-zero values of r_3, \dots, r_6 is due to smallness of the Wilson coefficients of the corresponding operators. In ref. [4], this effect was estimated to be around 1%. For that reason, the NLO QCD computation was called “practically complete” already at that time. However, it becomes *strictly complete* only now, when we learn exactly what the effect is and in what direction it acts.

4 Example of a two-loop diagram calculation: G_3

In the present section, we describe in detail the calculation of the two diagrams denoted by G_3 in fig. 1. We choose $(\bar{s}_L \gamma_\mu c_L)(\bar{c}_L \gamma^\mu b_L)$ for the inserted operator. Here, contrary to refs. [1, 2], no expansion in z is performed, because the limit $z \rightarrow 1$ is relevant for operators that contain three b -quarks. The UV divergences are regularized dimensionally. We treat γ_5 as fully anticommuting in $D = 4 - 2\epsilon$ dimensions. The s -quark is assumed to be massless.

The considered Feynman integral can be written as follows

$$G_3^{(1)} = \int \frac{d^D k}{k^2(q+k)^2} \bar{s} \gamma^\nu (\not{q} + \not{k}) \gamma_\rho P_L J_{\mu\nu} e^\mu \gamma^\rho P_L b, \quad (4.1)$$

where

$$J_{\mu\nu} = \int \frac{d^D p}{\Delta} \left\{ [\not{p} + \not{k} + m_c] \gamma_\nu [\not{p} + m_c] \gamma_\mu [\not{p} + \not{r} + m_c] - [\not{p} + \not{r} - m_c] \gamma_\mu [\not{p} - m_c] \gamma_\nu [\not{p} + \not{k} - m_c] \right\} \quad (4.2)$$

and

$$\Delta = [(p+k)^2 - m_c^2][(p+r)^2 - m_c^2][p^2 - m_c^2]. \quad (4.3)$$

Here, r and q stand for the outgoing photon and s -quark momenta, respectively. The momentum p runs inside the c -quark loop, while k is the gluon momentum. The polarization vector of the photon is denoted by e^μ .

Let us first consider the one-loop subgraph $J_{\mu\nu}$ for arbitrary off-shell momenta of the quarks, the gluon and the photon. The necessary one-loop integrals read

$$\int d^D p / \Delta \equiv a, \quad (4.4)$$

$$\int d^D p p_\alpha / \Delta = b k_\alpha + c r_\alpha, \quad (4.5)$$

$$\int d^D p p_\alpha p_\beta / \Delta = d m_c^2 g_{\alpha\beta} + e k_\alpha k_\beta + f r_\alpha r_\beta + g (k_\alpha r_\beta + r_\alpha k_\beta). \quad (4.6)$$

There is no need to consider $p_\alpha p_\beta p_\gamma$ in the numerator, because $\not{p}\gamma_\nu\not{p}\gamma_\mu\not{p}-\not{p}\gamma_\mu\not{p}\gamma_\nu\not{p}=p^2(\not{p}\gamma_\mu\gamma_\nu-\gamma_\nu\gamma_\mu\not{p})$. The coefficients a, \dots, g are not all independent. The following relations can be found by considering various contractions of the tensor integrals:

$$b = -\frac{1}{2}a - c - 2g - (c + 2f)\frac{k \cdot r}{k^2}, \quad (4.7)$$

$$d = \frac{1}{8\epsilon m_c^2} \left[a(k^2 - 4m_c^2) + 2c(k \cdot r + k^2 - 3r^2) + 4f(k \cdot r - 2r^2) + 4g(k^2 - 2k \cdot r) \right], \quad (4.8)$$

$$e = \frac{1}{4}a + \frac{1}{2}c + g + (c + 2f)\frac{k \cdot r + r^2}{2k^2}. \quad (4.9)$$

After performing the Dirac algebra with the above relations taken into account, one arrives at the following result:

$$J_{\mu\nu} = bV_{\mu\nu}^b + cV_{\mu\nu}^c + fV_{\mu\nu}^f + gV_{\mu\nu}^g + m_c \left[aP_{\mu\nu}^a + (c + 2f)P_{\mu\nu}^{cf} + gP_{\mu\nu}^g \right], \quad (4.10)$$

where

$$\begin{aligned} V_{\mu\nu}^b &= 2 \left(X_{\mu\nu}^{(2)} - X_{\mu\nu}^{(3)} \right), \\ V_{\mu\nu}^c &= 4 \left(\widetilde{X}_{\mu\nu}^{(3)} - \widetilde{X}_{\mu\nu}^{(2)} \right) + \frac{2r^2}{k^2} \left(X_{\mu\nu}^{(2)} - X_{\mu\nu}^{(3)} \right), \\ V_{\mu\nu}^f &= 4 \left(\widetilde{X}_{\mu\nu}^{(3)} - \widetilde{X}_{\mu\nu}^{(2)} \right) + \frac{4r^2}{k^2} \left(X_{\mu\nu}^{(2)} - X_{\mu\nu}^{(3)} \right), \\ V_{\mu\nu}^g &= 4 \left[(\not{r} - \not{k}) X_{\mu\nu}^{(1)} + X_{\mu\nu}^{(4)} - \widetilde{X}_{\mu\nu}^{(4)} \right], \\ P_{\mu\nu}^a &= 2 \left(X_{\mu\nu}^{(5)} - X_{\mu\nu}^{(6)} \right), \\ P_{\mu\nu}^{cf} &= -\frac{4}{k^2} X_{\mu\nu}^{(7)}, \\ P_{\mu\nu}^g &= -8 X_{\mu\nu}^{(1)}, \end{aligned} \quad (4.11)$$

and

$$\begin{aligned}
X_{\mu\nu}^{(1)} &= k \cdot r g_{\mu\nu} - k_\mu r_\nu, \\
X_{\mu\nu}^{(2)} &= \not{k}(k^2 g_{\mu\nu} - k_\mu k_\nu) - \gamma_\mu(k^2 r_\nu - k \cdot r k_\nu), \\
X_{\mu\nu}^{(3)} &= i(k^2 \gamma_\nu - \not{k} k_\nu) \sigma_{\alpha\mu} r^\alpha, \\
X_{\mu\nu}^{(4)} &= i(k \cdot r \gamma_\mu - \not{k} k_\mu) \sigma_{\alpha\nu} k^\alpha, \\
X_{\mu\nu}^{(5)} &= \sigma_{\alpha\nu} k^\alpha \sigma_{\beta\mu} r^\beta, \\
X_{\mu\nu}^{(6)} &= i \left[\sigma_{\mu\nu} k \cdot r - \sigma_{\alpha\beta} k^\alpha r^\beta g_{\mu\nu} + \sigma_{\alpha\mu} k^\alpha r_\nu - \sigma_{\alpha\nu} r^\alpha k_\mu \right], \\
X_{\mu\nu}^{(7)} &= k^2 r^2 g_{\mu\nu} - r^2 k_\mu k_\nu - k^2 r_\mu r_\nu + k \cdot r k_\nu r_\mu.
\end{aligned} \tag{4.12}$$

The structures $\widetilde{X}_{\mu\nu}^{(n)}$ are obtained from $X_{\mu\nu}^{(n)}$ by interchanging $\mu \leftrightarrow \nu$ and $k \leftrightarrow r$, i.e. $\widetilde{X}_{\mu\nu}^{(n)}(k, r) = X_{\nu\mu}^{(n)}(r, k)$. Note that each of those structures vanishes under contractions with k^ν and r^μ . This is a manifestation of the Ward identities $k^\nu J_{\mu\nu} = r^\mu J_{\mu\nu} = 0$.

Once we have found the one-loop integral $J_{\mu\nu}$, we should complete the remaining Dirac algebra in $G_3^{(1)}$ (4.1). Given our explicit expressions for the structures $X_{\mu\nu}^{(k)}$ and $\widetilde{X}_{\mu\nu}^{(k)}$, it is easy to verify that

$$\gamma_\rho P_L J_{\mu\nu} \gamma^\rho P_L = (2 + 2\epsilon) P_R \left[b V_{\mu\nu}^b + c V_{\mu\nu}^c + f V_{\mu\nu}^f + g V_{\mu\nu}^g \right]. \tag{4.13}$$

Consequently, in our present calculation of the matrix element of $(\bar{s}_L \gamma_\mu c_L)(\bar{c}_L \gamma^\mu b_L)$, the terms proportional to m_c in $J_{\mu\nu}$ (4.10) are irrelevant. Nevertheless, we have presented them explicitly here because they matter for other operators.

From now on, we shall impose the on-shell conditions for the quarks and the photon: $q^2 = r^2 = 0$, $q \cdot r = \frac{1}{2} m_b^2$, $\bar{s} \not{q} = 0$ and $(\not{q} + \not{r})b = m_b b$. For an arbitrary scalar function $F(k^2, k \cdot r, k \cdot q)$, we find the following identities:

$$\begin{aligned}
\int d^D k F(k^2, k \cdot r, k \cdot q) \bar{s} \gamma^\nu (\not{q} + \not{k}) V_{\mu\nu}^b e^\mu b &= [\text{terms proportional to } \bar{s} \not{q} b \text{ and } (e \cdot r) \bar{s} b] \\
&+ m_b \bar{s} (\not{q} \not{r} - \not{r} \not{q}) b \int d^D k F(k^2, k \cdot r, k \cdot q) \left[(k + q)^2 \frac{k \cdot r}{m_b^2} - k^2 \left(1 + \frac{2k \cdot r}{m_b^2} \right) \right], \tag{4.14}
\end{aligned}$$

$$\int d^D k F(k^2, k \cdot r, k \cdot q) \bar{s} \gamma^\nu (\not{q} + \not{k}) V_{\mu\nu}^c e^\mu b = [\text{terms proportional to } \bar{s} \not{q} b \text{ and } (e \cdot r) \bar{s} b], \tag{4.15}$$

$$\int d^D k F(k^2, k \cdot r, k \cdot q) \bar{s} \gamma^\nu (\not{q} + \not{k}) V_{\mu\nu}^f e^\mu b = [\text{terms proportional to } \bar{s} \not{q} b \text{ and } (e \cdot r) \bar{s} b], \tag{4.16}$$

$$\begin{aligned}
\int d^D k F(k^2, k \cdot r, k \cdot q) \bar{s} \gamma^\nu (\not{q} + \not{k}) V_{\mu\nu}^g e^\mu b &= [\text{terms proportional to } \bar{s} \not{q} b \text{ and } (e \cdot r) \bar{s} b] \\
&+ \frac{m_b \bar{s} (\not{q} \not{r} - \not{r} \not{q}) b}{1 - \epsilon} \int d^D k F(k^2, k \cdot r, k \cdot q) \left[2\epsilon (k + q)^2 \frac{k \cdot r}{m_b^2} - k^2 \left(1 + (2 - 3\epsilon + 2\epsilon^2) \frac{2k \cdot r}{m_b^2} \right) \right]. \tag{4.17}
\end{aligned}$$

Consequently, $G_3^{(1)}$ (4.1) takes the following form

$$G_3^{(1)} = 4\Gamma(1+2\epsilon)\pi^D m_b^{-4\epsilon} \bar{s}P_R \left\{ R_3^{(1)} m_b (\not{\epsilon} \not{r} - \not{r} \not{\epsilon}) + R_3'^{(1)} m_b e \cdot r + R_3''^{(1)} \not{\epsilon} \right\} b, \quad (4.18)$$

where

$$R_3^{(1)} = \frac{(1+\epsilon)m_b^{4\epsilon}}{2\Gamma(1+2\epsilon)\pi^D} \int \frac{d^D k}{k^2(k+q)^2} \left\{ b(k^2, k \cdot r) \left[(k+q)^2 \frac{k \cdot r}{m_b^2} - k^2 \left(1 + \frac{2k \cdot r}{m_b^2} \right) \right] \right. \\ \left. + \frac{g(k^2, k \cdot r)}{1-\epsilon} \left[2\epsilon(k+q)^2 \frac{k \cdot r}{m_b^2} - k^2 \left(1 + (2-3\epsilon+2\epsilon^2) \frac{2k \cdot r}{m_b^2} \right) \right] \right\}. \quad (4.19)$$

As discussed in the next section, we do not need to calculate $R_3'^{(1)}$ and $R_3''^{(1)}$. The overall normalization factor in eq. (4.18) is chosen in such a manner that the $\mathcal{O}(1)$ part of $R_3^{(1)}$ is equal to the quantity \widetilde{M}_3 from our previous article [1] (see eqs. (2.6) and (2.11) there).

The terms proportional to $(k+q)^2 k \cdot r$ in the curly bracket of eq. (4.19) give vanishing integrals over k . Consequently, $R_3^{(1)}$ simplifies to

$$R_3^{(1)} = -\frac{(1+\epsilon)m_b^{4\epsilon}}{2\Gamma(1+2\epsilon)\pi^D} \int \frac{d^D k}{(k+q)^2 + i\varepsilon} \left[\left(1 + \frac{2k \cdot r}{m_b^2} \right) b + \left(1 + (2-3\epsilon+2\epsilon^2) \frac{2k \cdot r}{m_b^2} \right) \frac{g}{1-\epsilon} \right]. \quad (4.20)$$

Now, we need explicit expressions for b and g . They can be easily found from eqs. (4.5) and (4.6) with the help of Feynman parameters

$$b(k^2, k \cdot r) = i\pi^{D/2}\Gamma(1+\epsilon) \int_0^1 dx \int_0^1 dy \frac{x^{-\epsilon}(1-x)^{-\epsilon}}{[-(k-yr)^2 + \frac{m_c^2 - i\varepsilon}{x(1-x)}]^{1+\epsilon}}, \quad (4.21)$$

$$g(k^2, k \cdot r) = i\pi^{D/2}\Gamma(1+\epsilon) \int_0^1 dx \int_0^1 dy \frac{x^{-\epsilon}(1-x)^{-\epsilon}}{[-(k-yr)^2 + \frac{m_c^2 - i\varepsilon}{x(1-x)}]^{1+\epsilon}} (-xy). \quad (4.22)$$

Introducing another Feynman parameter and integrating over k , one obtains

$$R_3^{(1)} = -\frac{1+\epsilon}{4\epsilon(1-\epsilon)} \int_0^1 dx \int_0^1 dy \int_0^1 dv \frac{(1-\epsilon)v + xy[(1-v)(2-3\epsilon+2\epsilon^2) - 1]}{x^{-\epsilon}(1-x)^{-\epsilon} v^\epsilon [z - i\varepsilon - x(1-x)y(1-v)]^{2\epsilon}}, \quad (4.23)$$

where $z = m_c^2/m_b^2$. After expanding the integrand to $\mathcal{O}(\epsilon)$ and performing the easy integrations, we find

$$R_3^{(1)} = -\frac{1}{8\epsilon} + \frac{1}{8} + \frac{1}{2} \int_0^1 dx \int_0^1 dy \int_0^1 dv [1-v + xy(2v-1)] \ln[z - i\varepsilon - x(1-x)yv]. \quad (4.24)$$

In the next section, analogous results for all the diagrams in fig. 1 will be presented.

5 Results for the unrenormalized two-loop diagrams

In the present section, we shall be interested in the *unrenormalized* two-loop 1PI on-shell $b \rightarrow s\gamma$ diagrams with insertions of the following 4-quark operators:

$$Q^{(n)} = \frac{1}{4^{n-1}} (\bar{s} P_R \gamma_{\alpha_1} \dots \gamma_{\alpha_n} c) (\bar{c} \gamma^{\alpha_n} \dots \gamma^{\alpha_1} P_L b), \quad (5.1)$$

$$\tilde{Q}^{(n)} = \frac{1}{4^{n-1}} (\bar{s} P_R \gamma_{\alpha_1} \dots \gamma_{\alpha_n} c) (\bar{c} \gamma^{\alpha_n} \dots \gamma^{\alpha_1} P_R b). \quad (5.2)$$

The corresponding diagrams in fig. 1 will be denoted by $G_k^{(n)}$ and $\tilde{G}_k^{(n)}$, respectively. Their overall normalization is assumed to be the same as in eq. (4.1), e.g.

$$\tilde{G}_3^{(n)} = \frac{1}{4^{n-1}} \int \frac{d^D k}{k^2 (q+k)^2} \bar{s} \gamma^\nu (\not{q} + \not{k}) P_R \gamma_{\alpha_1} \dots \gamma_{\alpha_n} J_{\mu\nu} e^\mu \gamma^{\alpha_n} \dots \gamma^{\alpha_1} P_R b. \quad (5.3)$$

The operators $Q^{(0)}$, $Q^{(1)}$, $\tilde{Q}^{(0)}$, $\tilde{Q}^{(1)}$, $\tilde{Q}^{(2)}$ together with their mirror copies and analogous operators with color-octet currents form a complete set of dimension-six $(\bar{s}c)(\bar{c}b)$ operators in four spacetime dimensions. Extending our results to $\Delta B = -\Delta S = 1$ four-quark operators with other flavor contents is straightforward, as we perform no expansion in the ratio m_c/m_b .

For the operators $Q^{(n)}$, only the diagrams $G_1^{(n)}$, ..., $G_4^{(n)}$ matter. The remaining ones in fig. 1 vanish due to chirality conservation in the charm-quark loop and QED gauge invariance.

For $\tilde{Q}^{(n)}$, the set $\tilde{G}_7^{(n)}$ gives no contribution on-shell, i.e. it cancels with the corresponding 1PR diagrams, because it is proportional to the matrix element of a two-quark operator $\bar{s} P_R b$ that vanishes by the equations of motion, up to a total derivative

$$\bar{s} P_R b = -\frac{1}{m_b} \left[\bar{s} P_R (\not{D} - m_b) b + \bar{s} \overleftarrow{\not{D}} P_L b - \partial^\mu (\bar{s} \gamma_\mu P_L b) \right]. \quad (5.4)$$

The diagram $\tilde{G}_6^{(n)}$ is just a product of two one-loop diagrams. It contains an IR divergence that cancels out only after adding the corresponding bremsstrahlung corrections. However, for all the $\tilde{Q}^{(n)}$ except $\tilde{Q}^{(0)}$ (which is of no interest in the SM), the effect of those diagrams can be taken into account by the standard replacement $C_7 \rightarrow C_7^{\text{eff}}$ (see section 6). Thus, we shall ignore $\tilde{G}_6^{(n)}$ in this section, i.e. we shall consider only $\tilde{G}_1^{(n)}$, ..., $\tilde{G}_5^{(n)}$ for the operators $\tilde{Q}^{(n)}$.

By analogy to eq. (4.18), we write

$$G_k^{(n)} = 4\Gamma(1+2\epsilon)\pi^D m_b^{-4\epsilon} \bar{s} P_R \left\{ R_k^{(n)} m_b (\not{\epsilon}' - \not{\epsilon}) + R_k'^{(n)} m_b e \cdot r + R_k''^{(n)} \not{\epsilon}' \right\} b, \quad (5.5)$$

and similarly for $\tilde{G}_k^{(n)}$. Below, we shall present our results for the coefficients in front of $(\not{\epsilon}' - \not{\epsilon})$ only. Due to QED gauge invariance, the remaining Dirac structures must cancel out when all the 1PI and 1PR diagrams are included. No explicit calculation of the 1PR diagrams is necessary, as they can give no $(\not{\epsilon}' - \not{\epsilon})$ structure.

We have found the following expressions for $R_k^{(n)}$ and $\tilde{R}_k^{(n)}$:

$$R_1^{(1)} = \frac{1}{36\epsilon} - \frac{1}{18} \ln z - \frac{2}{3} z^2 - \frac{47}{18} z + \frac{37}{216} + \frac{12z^2 + 16z - 1}{18} \sqrt{1-4z} f(z) + \frac{z^2(2z-3)}{3} f(z)^2, \quad (5.6)$$

$$R_2^{(1)} = -\frac{5}{36\epsilon} + \frac{35}{72} - \frac{1}{2} z + \int_0^1 dx \int_0^1 dy \frac{\frac{1}{2} y^2 (y^2 - 1) x (1-x) + (2-y) u_1 \ln u_1 + (2y^2 - 2y - 1) u_2 \ln u_2}{(1-y)^2}, \quad (5.7)$$

$$R_3^{(1)} = -\frac{1}{8\epsilon} + \frac{1}{8} + \frac{1}{2} \int_0^1 dx \int_0^1 dy \int_0^1 dv [1 - v + xy(2v - 1)] \ln[z - i\epsilon - x(1-x)vy], \quad (5.8)$$

$$R_4^{(1)} = -\frac{1}{4\epsilon} + \frac{3}{4} + \frac{1}{2} \int_0^1 dx \int_0^1 dy \int_0^1 dv [2 - v + xy(2v - 3)] \ln[vz + x(1-x)(1-v)(1-v+vy)], \quad (5.9)$$

$$\tilde{R}_1^{(1)} = \sqrt{z} \left\{ -\frac{1}{4\epsilon} - \frac{11+4i\pi}{8} + \epsilon \left[\frac{10\pi^2 - 85 - 44i\pi}{16} + \int_0^1 dx \int_0^1 dy \int_0^1 dv \frac{v}{y} \ln \left(1 - \frac{yz}{x(1-x)(1-v)} + i\epsilon \right) \right] \right\}, \quad (5.10)$$

$$\tilde{R}_2^{(1)} = \sqrt{z} \left\{ -\frac{1}{4\epsilon} + \frac{4\pi^2 - 51}{24} + \epsilon \left[\frac{6\pi^2 - 171 + 80\zeta(3)}{16} + \int_0^1 dx \int_0^1 dy \left(\frac{y-3}{2-2y} \text{Li}_2(w_1) + \frac{y(3-2y)}{1-y} \text{Li}_2(w_2) \right) \right] \right\}, \quad (5.11)$$

$$\tilde{R}_3^{(n)} = \sqrt{z} \begin{cases} \frac{n-2}{4\epsilon} - \frac{n-2}{2} \ln z - \frac{n}{8} + 1 + z - \frac{2z+1}{2} \sqrt{1-4z} f(z) + z(1-z)f(z)^2, & \text{n odd,} \\ Y^{(n)} + \int_0^1 dx \int_0^1 dy \int_0^1 dv \left\{ \frac{1-2x^2y}{x} \ln [z - x(1-x)vy - i\epsilon] - \frac{1}{x} \ln z \right\}, & \text{n even,} \end{cases} \quad (5.12)$$

$$\tilde{R}_4^{(n)} = \sqrt{z} \begin{cases} \frac{n-2}{4\epsilon} + \frac{3-n}{2} \ln z - \frac{n+6}{8} - 2 \int_0^1 dx \int_0^1 dy \int_0^1 dv xy \ln \frac{zv+x(1-x)(1-v)(1-v+vy)}{v}, & \text{n odd,} \\ Y^{(n)} + \int_0^1 dx \int_0^1 dy \int_0^1 dv \left\{ \frac{1-2x^2y}{x} \ln \frac{zv+x(1-x)(1-v)(1-v+vy)}{v} - \frac{1}{x} \ln z \right\}, & \text{n even,} \end{cases} \quad (5.13)$$

$$\tilde{R}_5^{(1)} = \frac{\sqrt{z}}{4} \left[\frac{1}{\epsilon} - 2 \ln z - \frac{5}{2} + \epsilon \left(\frac{3}{4} - \frac{\pi^2}{6} + 5 \ln z + 2 \ln^2 z \right) \right], \quad (5.14)$$

where $Y^{(n)} = -\frac{1}{2\epsilon^2} + \frac{1}{\epsilon} \left(\ln z + \frac{1}{4} \right) - \ln^2 z + \frac{\pi^2}{12} - \frac{n^2-5n+6}{16}$ and $w_k = \frac{(y-1)z}{x(1-x)y^k}$. The variables u_k and the function $f(z)$ are as in $b(z)$ in eq. (3.4).

We have presented $\tilde{R}_3^{(n)}$ and $\tilde{R}_4^{(n)}$ for arbitrary n , while $n = 1$ was assumed otherwise. In those cases, results for other n can be found from the following simple relations:

$$G_k^{(n+1)} = \begin{cases} \frac{-1+\epsilon}{2} G_k^{(n)}, & \text{for } k = 1, 2, & (\text{because } \gamma_\alpha \gamma_\mu \gamma^\alpha = (-2 + 2\epsilon) \gamma_\mu), \\ \frac{+1+\epsilon}{2} G_k^{(n)}, & \text{for } k = 3, 4, & (\text{see eq. (4.13)}), \end{cases} \quad (5.15)$$

$$\tilde{G}_k^{(n+1)} = -\frac{\epsilon}{2} \tilde{G}_k^{(n)}, \quad \text{for } k = 1, 2, 5, \quad (\text{because } \gamma_\alpha \sigma_{\mu\nu} \gamma^\alpha = -2\epsilon \sigma_{\mu\nu}). \quad (5.16)$$

The overall factor of ϵ in the r.h.s. of the latter equation is the reason why we have calculated the $\mathcal{O}(\epsilon)$ parts of $\tilde{R}_1^{(1)}$, $\tilde{R}_2^{(1)}$ and $\tilde{R}_5^{(1)}$. They are necessary for the $\mathcal{O}(1)$ matrix elements of $\tilde{Q}^{(0)}$, i.e. they may matter beyond SM.

For the color-octet analogues of $Q^{(n)}$ and $\tilde{Q}^{(n)}$, the expressions for $R_k^{(n)}$ and $\tilde{R}_k^{(n)}$ get multiplied by additional color factors of $-\frac{1}{6}$ (for $k \leq 4$) and $\frac{4}{3}$ (otherwise). Of course, the values of $R_k^{(n)}$ and $\tilde{R}_k^{(n)}$ remain the same for the mirror copies of $Q^{(n)}$ and $\tilde{Q}^{(n)}$, provided P_R is replaced by P_L in eq. (5.5).

Thus, apart from the trivial case of $\tilde{G}_6^{(n)}$, the present section contains complete results for the unrenormalized two-loop $b \rightarrow s\gamma$ diagrams with insertions of four-quark operators, in the SM and beyond.⁴

6 The $\overline{\text{MS}}$ -renormalized amplitude in the SM

In the present section, we shall restrict ourselves to the SM operators P_k (2.2) and use eqs. (5.6)–(5.14) to evaluate the $\overline{\text{MS}}$ -renormalized on-shell $b \rightarrow s\gamma$ amplitude at the NLO in QCD. From this amplitude one reads out the coefficients r_k , i.e. our main results presented in section 3.

The renormalized effective Lagrangian reads⁵

$$\begin{aligned} \mathcal{L}_{\text{eff}} = & \mathcal{L}_{\text{QCD} \times \text{QED}} + \frac{4G_F}{\sqrt{2}} V_{ts}^* V_{tb} \left\{ C_7(\mu) Z_{77} Z_\psi Z_m P_7 + C_8(\mu) Z_\psi Z_m \left(Z_{88} Z_g Z_G^{\frac{1}{2}} P_8 + Z_{87} P_7 \right) \right. \\ & \left. + \sum_{k=1}^6 C_k(\mu) \left[Z_\psi^2 \left(\sum_{j=1}^6 Z_{kj} P_j + \sum_{j=3}^4 Z_{kj}^E E_j^{(1)} \right) + Z_{k7} Z_\psi Z_m P_7 \right] \right\} + \dots \end{aligned} \quad (6.1)$$

The evanescent operators $E_3^{(1)}$ and $E_4^{(1)}$ are as in the appendix of ref. [7]

$$\begin{aligned} E_3^{(1)} &= (\bar{s}_L \gamma_{\mu_1} \gamma_{\mu_2} \gamma_{\mu_3} \gamma_{\mu_4} \gamma_{\mu_5} b_L) \sum_q (\bar{q} \gamma^{\mu_1} \gamma^{\mu_2} \gamma^{\mu_3} \gamma^{\mu_4} \gamma^{\mu_5} q) - 20P_5 + 64P_3, \\ E_4^{(1)} &= (\bar{s}_L \gamma_{\mu_1} \gamma_{\mu_2} \gamma_{\mu_3} \gamma_{\mu_4} \gamma_{\mu_5} T^a b_L) \sum_q (\bar{q} \gamma^{\mu_1} \gamma^{\mu_2} \gamma^{\mu_3} \gamma^{\mu_4} \gamma^{\mu_5} T^a q) - 20P_6 + 64P_4. \end{aligned} \quad (6.2)$$

The dots in eq. (6.1) stand for other evanescent operators that do not affect the NLO matrix elements. They are relevant for the NLO anomalous dimension matrix though.

Below, in the calculation of the $\overline{\text{MS}}$ -renormalized amplitude, we shall use the $\overline{\text{MS}}$ -scheme renormalization constants, and implicitly assume that all the unrenormalized l -loop matrix elements are multiplied by $(4\pi)^{-l\epsilon} e^{l\epsilon\gamma}$. The light (u, d, s) quark masses will be neglected.

In the NLO calculation of $b \rightarrow s\gamma$ matrix elements, the renormalization constants Z_g and Z_G can be set to unity. As far as Z_m and Z_ψ are concerned, we need the one-loop expressions $Z_m = 1 - \frac{\alpha_s}{\pi\epsilon}$ and $Z_\psi = 1 - \frac{\alpha_s}{3\pi\epsilon}$.

⁴ Up to operators that vanish in 4 spacetime dimensions, i.e. evanescent operators — see section 6.

⁵ Note that the interaction terms in eq. (2.1) have opposite sign.

The renormalization constants Z_{k3}^E and Z_{k4}^E can be found from eqs. (20)⁶ and (45) of ref. [7]. The only non-vanishing contributions to those constants at order $\mathcal{O}(\alpha_s)$ are $Z_{54}^E = \frac{\alpha_s}{4\pi\epsilon}$, $Z_{63}^E = \frac{\alpha_s}{18\pi\epsilon}$ and $Z_{64}^E = \frac{5\alpha_s}{48\pi\epsilon}$.

The renormalization constants Z_{kj} can be found from the anomalous dimension matrix $\hat{\gamma}^{(0)\text{eff}}$ given in eq. (8) of ref. [4]⁷

$$\hat{\gamma}^{(0)\text{eff}} = \begin{bmatrix} -4 & \frac{8}{3} & 0 & -\frac{2}{9} & 0 & 0 & -\frac{208}{243} & \frac{173}{162} \\ 12 & 0 & 0 & \frac{4}{3} & 0 & 0 & \frac{416}{81} & \frac{70}{27} \\ 0 & 0 & 0 & -\frac{52}{3} & 0 & 2 & -\frac{176}{81} & \frac{14}{27} \\ 0 & 0 & -\frac{40}{9} & -\frac{100}{9} & \frac{4}{9} & \frac{5}{6} & -\frac{152}{243} & -\frac{587}{162} \\ 0 & 0 & 0 & -\frac{256}{3} & 0 & 20 & -\frac{6272}{81} & \frac{6596}{27} \\ 0 & 0 & -\frac{256}{9} & \frac{56}{9} & \frac{40}{9} & -\frac{2}{3} & \frac{4624}{243} & \frac{4772}{81} \\ 0 & 0 & 0 & 0 & 0 & 0 & \frac{32}{3} & 0 \\ 0 & 0 & 0 & 0 & 0 & 0 & -\frac{32}{9} & \frac{28}{3} \end{bmatrix}. \quad (6.3)$$

The relation $Z_{kj} = \delta_{kj} + \frac{\alpha_s}{8\pi\epsilon} \gamma_{kj}^{(0)\text{eff}}$ holds for all the Z_{kj} except $(Z_{k7}, Z_{k8})_{k=1,\dots,6}$. In the latter case,

$$Z_{k7} = \frac{\alpha_s}{16\pi\epsilon} \gamma_{k7}^{(0)} - \frac{1}{2} \sum_{j=3}^4 Z_{kj}^E y_j^E, \quad (6.4)$$

where $\hat{\gamma}$ is related to $\hat{\gamma}^{\text{eff}}$ by [5]

$$\gamma_{ji}^{\text{eff}} = \begin{cases} \gamma_{j7} + \sum_{k=1}^6 y_k \gamma_{jk} - y_j \gamma_{77} - z_j \gamma_{87}, & \text{when } i = 7 \text{ and } j = 1, \dots, 6, \\ \gamma_{j8} + \sum_{k=1}^6 z_k \gamma_{jk} - z_j \gamma_{88}, & \text{when } i = 8 \text{ and } j = 1, \dots, 6, \\ \gamma_{ji}, & \text{otherwise,} \end{cases} \quad (6.5)$$

with y_i and z_i given in eq. (2.4). The numbers y_k and y_j^E parametrize the unrenormalized on-shell one-loop $b \rightarrow s\gamma$ matrix elements of the 4-quark operators

$$\langle P_k \rangle_{1\text{ loop}} = \left(\frac{\mu}{m_b} \right)^{2\epsilon} \tilde{y}_k \langle P_7 \rangle_{\text{tree}} + \mathcal{O}(\epsilon^2), \quad (y_k = \lim_{\epsilon \rightarrow 0} \tilde{y}_k), \quad (6.6)$$

$$\langle E_j^{(1)} \rangle_{1\text{ loop}} = \left(\frac{\mu}{m_b} \right)^{2\epsilon} \tilde{y}_j^E \langle P_7 \rangle_{\text{tree}} + \mathcal{O}(\epsilon^2), \quad (y_j^E = \lim_{\epsilon \rightarrow 0} \tilde{y}_j^E). \quad (6.7)$$

An easy one-loop calculation gives $\tilde{y}_1 = \tilde{y}_2 = 0$ and

$$\begin{aligned} \tilde{y}_3 &= Q_d = -\frac{1}{3}, & \tilde{y}_4 &= Q_d C_F = -\frac{4}{9}, \\ \tilde{y}_5 &= 4(5 - 3\epsilon)Q_d, & \tilde{y}_6 &= 4(5 - 3\epsilon)Q_d C_F, \\ \tilde{y}_3^E &= 16(4 - 25\epsilon)Q_d, & \tilde{y}_4^E &= 16(4 - 25\epsilon)Q_d C_F. \end{aligned} \quad (6.8)$$

⁶ In that equation, the expression “(counterterms due to Z_ψ^2)” has been missed.

⁷ Signs of $\gamma_{k7}^{(0)\text{eff}}$ and $\gamma_{k8}^{(0)\text{eff}}$ are fixed by our sign convention inside $D_\mu \psi = (\partial_\mu + igG_\mu^a T^a + ieQA_\mu) \psi$.

The unrenormalized one-loop matrix elements of P_7 and P_8 can be expressed as follows:

$$\langle P_7 \rangle_{1 \text{ loop}} = \frac{\alpha_s}{4\pi} \tilde{r}_7 \langle P_7 \rangle_{\text{tree}}, \quad (6.9)$$

$$\langle P_8 \rangle_{1 \text{ loop}} = \left(\frac{\mu}{m_b} \right)^{2\epsilon} \left(-Z_{87} + \frac{\alpha_s}{4\pi} r_8 \right) \langle P_7 \rangle_{\text{tree}} + \mathcal{O}(\alpha_s^2, \epsilon). \quad (6.10)$$

No explicit expression for \tilde{r}_7 is necessary for our purpose. It is enough to mention that \tilde{r}_7 is UV-finite (note that $Z_{77}Z_\psi Z_m = 1 + \mathcal{O}(\alpha_s^2)$), but it contains an IR divergence. We assume that this IR divergence is regulated with a small gluon mass.

The quantity r_8 reads [2]

$$r_8 = \frac{44}{9} - \frac{8}{27}\pi^2 + \frac{8}{9}i\pi. \quad (6.11)$$

We have verified this result during the calculation of $\tilde{R}_1^{(1)}$ and $\tilde{R}_2^{(1)}$.

In the following, we shall need two unrenormalized matrix elements of evanescent operators

$$\langle P_4^{c\bar{c}} + \frac{1}{6}P_3^{c\bar{c}} - \frac{1}{2}Q^{(1)} + \frac{1}{4}Q^{(0)} \rangle_{2 \text{ loop}} = \frac{\alpha_s}{4\pi} e_4 \langle P_7 \rangle_{\text{tree}} + \mathcal{O}(\epsilon), \quad (6.12)$$

$$\langle P_6^{c\bar{c}} + \frac{1}{6}P_5^{c\bar{c}} - 8Q^{(1)} + Q^{(0)} \rangle_{2 \text{ loop}} = \frac{\alpha_s}{4\pi} e_6 \langle P_7 \rangle_{\text{tree}} + \mathcal{O}(\epsilon), \quad (6.13)$$

where $P_k^{c\bar{c}}$ are just the $c\bar{c}$ -parts of the respective P_k . Note that $\langle P_3^{c\bar{c}} \rangle_{2 \text{ loop}} = \langle P_5^{c\bar{c}} \rangle_{2 \text{ loop}} = 0$ due to color factors. We find $e_4 = Q_u - \frac{8}{27}Q_d$ and $e_6 = 16Q_u - \frac{32}{27}Q_d$. These results are independent of m_c . Thus, after appropriate replacement of quark charges, they hold for any flavor circulating in the loop. Consequently, we can use eqs. (6.12) and (6.13) to express all the two-loop diagrams with Dirac traces in $\langle P_k \rangle_{2 \text{ loop}}$ as linear combinations of the results from section 5, up to the following additive constants obtained from e_4 and e_6 :

$$D_4 = uQ_u + dQ_d - \frac{8}{27}(u+d)Q_d, \quad \text{and} \quad D_6 = 16(uQ_u + dQ_d) - \frac{32}{27}(u+d)Q_d, \quad (6.14)$$

where $u = 2$ and $d = 3$ are the numbers of active up and down flavors, respectively.

Such an approach is much more convenient than calculating diagrams with Dirac traces separately, because e_4 and e_6 can be (and are) found using expansion in external momenta and computer algebra, as in the so-called matching computations (see e.g. ref. [8]). More precisely, such an expansion is applied to diagrams with subtracted subdivergences, because subtracted matrix elements of evanescent operators must be local (i.e. polynomial in external momenta). Once they are found, we add the one-loop subdivergences again, setting the external momenta on shell. Then, the only relevant subdivergence is proportional to $\langle P_4 \rangle_{1 \text{ loop}}$ that we already know.

Now, we are ready to calculate the unrenormalized two-loop matrix elements of P_k . Let us write them as follows:

$$\langle P_k \rangle_{2 \text{ loop}} = \frac{\alpha_s}{4\pi} \left(\frac{\mu}{m_b} \right)^{4\epsilon} (x_k + \tilde{r}_7 \tilde{y}_k) \langle P_7 \rangle_{\text{tree}} + \mathcal{O}(\epsilon), \quad (6.15)$$

where the terms proportional to \tilde{r}_7 originate from $\tilde{G}_6^{(n)}$ diagrams. Evaluation of x_k amounts to forming appropriate linear combinations of eqs. (5.6)–(5.14) with $z \rightarrow 0, z$ or 1 , according to the Dirac and flavor structure of P_k . Explicitly

$$\begin{aligned}
x_1 &= -\frac{1}{6} \left[Q_d H_{12}^{(1)}(z) + Q_u H_{34}^{(1)}(z) \right], \\
x_2 &= Q_d H_{12}^{(1)}(z) + Q_u H_{34}^{(1)}(z), \\
x_3 &= Q_d \left[H_{14}^{(1)}(0) + H_{14}^{(1)}(1) + \widetilde{H}_{15}^{(1)} \right], \\
x_4 &= D_4 + Q_u [H'_{34}(0) + H'_{34}(z)] + Q_d [3H'_{12}(0) + 2H'_{34}(0) + H'_{12}(z) + H'_{14}(1) \\
&\quad - \frac{1}{6} (H_{14}^{(1)}(0) + H_{14}^{(1)}(1) + \widetilde{H}_{14}^{(1)}) + C_F Q_d \widetilde{H}_{55}^{(1)}], \\
x_5 &= Q_d \left[H_{14}^{(3)}(0) + H_{14}^{(3)}(1) + \widetilde{H}_{15}^{(3)} \right], \\
x_6 &= D_6 + Q_u [H''_{34}(0) + H''_{34}(z)] + Q_d [3H''_{12}(0) + 2H''_{34}(0) + H''_{12}(z) + H''_{14}(1) \\
&\quad - \frac{1}{6} (H_{14}^{(3)}(0) + H_{14}^{(3)}(1) + \widetilde{H}_{14}^{(3)}) + C_F Q_d \widetilde{H}_{55}^{(3)}], \tag{6.16}
\end{aligned}$$

where

$$\begin{aligned}
H_{ij}^{(n)}(y) &= 4^n C_F \sum_{k=i}^j S_k^{(n)}(y), & \widetilde{H}_{ij}^{(n)} &= 4^n C_F \sum_{k=i}^j \widetilde{S}_k^{(n)}, \\
H'_{ij}(y) &= \frac{1}{2} H_{ij}^{(1)}(y) - H_{ij}^{(0)}(y), & H''_{ij}(y) &= 8H_{ij}^{(1)}(y) - 4H_{ij}^{(0)}(y), \\
S_i^{(n)}(y) &= \begin{cases} (R_i^{(n)})_{z \rightarrow y}, & n = 0, 1, \\ [-R_i^{(3)} + (20 - 12\epsilon)R_i^{(1)}]_{z \rightarrow y}, & n = 3. \end{cases} \tag{6.17}
\end{aligned}$$

The relations between $\widetilde{S}_i^{(n)}$ and $(\widetilde{R}_i^{(n)})_{z \rightarrow 1}$ are the same as between $S_i^{(n)}(1)$ and $(R_i^{(n)})_{z \rightarrow 1}$. The necessity of introducing $S_i^{(n)}$ and $\widetilde{S}_i^{(n)}$ follows from the fact that ordering of the Dirac matrices in P_5 and P_6 is opposite to the one in $Q^{(3)}$ and $\widetilde{Q}^{(3)}$.

After all the above substitutions, one finds (up to $\mathcal{O}(\epsilon)$)

$$\begin{aligned}
x_1 &= \frac{46}{243\epsilon} + \frac{833}{729} - \frac{1}{3}[a(z) + b(z)] + \frac{40}{243}i\pi, \\
x_2 &= -\frac{92}{81\epsilon} - \frac{1666}{243} + 2[a(z) + b(z)] - \frac{80}{81}i\pi, \\
x_3 &= \frac{248}{81\epsilon} + \frac{2932}{243} - \frac{8}{27}\pi^2 + \frac{8\pi}{3\sqrt{3}} + \frac{32}{9}X_b - a(1) + 2b(1) + \frac{128}{81}i\pi, \\
x_4 &= -\frac{46}{243\epsilon} - \frac{1031}{729} + \frac{4}{81}\pi^2 - \frac{4\pi}{9\sqrt{3}} - \frac{16}{27}X_b + \frac{1}{6}a(1) + \frac{5}{3}b(1) + 2b(z) - \frac{184}{243}i\pi, \\
x_5 &= \frac{5552}{81\epsilon} + \frac{42424}{243} - \frac{160}{27}\pi^2 + \frac{32\pi}{3\sqrt{3}} + \frac{128}{9}X_b - 16a(1) + 32b(1) + \frac{2336}{81}i\pi, \\
x_6 &= -\frac{4588}{243\epsilon} - \frac{14378}{729} + \frac{80}{81}\pi^2 - \frac{16\pi}{9\sqrt{3}} - \frac{64}{27}X_b - \frac{10}{3}a(1) + \frac{44}{3}b(1) + 12a(z) + 20b(z) - \frac{3016}{243}i\pi. \tag{6.18}
\end{aligned}$$

where the constant X_b as well as the functions $a(z)$ and $b(z)$ have been already defined in section 3.

Once we have found the unrenormalized matrix elements of P_1, \dots, P_6 , it is straightforward to calculate the renormalized ones. The $\overline{\text{MS}}$ -renormalized amplitude for $b \rightarrow s\gamma$ decay reads⁸

$$\begin{aligned}
M = & \left[C_7^{(0)}(\mu) + \frac{\alpha_s}{4\pi} C_7^{(1)}(\mu) \right] [\langle P_7 \rangle_{\text{tree}} + \langle P_7 \rangle_{1 \text{ loop}}] + C_8^{(0)}(\mu) [\langle P_8 \rangle_{1 \text{ loop}} + Z_{87} \langle P_7 \rangle_{\text{tree}}] \\
& + \sum_{k=1}^6 \left[C_k^{(0)}(\mu) + \frac{\alpha_s}{4\pi} C_k^{(1)}(\mu) \right] \left\{ \sum_{j=1}^6 [Z_{kj} Z_\psi + (1 - 2\epsilon)(Z_m - 1)\delta_{kj}] \langle P_j \rangle_{1 \text{ loop}} \right. \\
& \left. + \langle P_k \rangle_{2 \text{ loop}} + Z_{k7} \langle P_7 \rangle_{\text{tree}} + \sum_{j=3}^4 Z_{kj}^E \langle E_j^{(1)} \rangle_{1 \text{ loop}} \right\} + \mathcal{O}(\alpha_s^2, \epsilon). \tag{6.19}
\end{aligned}$$

When comparing the above equation with eq. (6.1), one should remember about the identity $Z_{77} Z_\psi Z_m = 1 + \mathcal{O}(\alpha_s^2)$.

The appearance of Z_ψ and Z_m in eq. (6.19) can be understood without calculating any diagram. It is enough to remember that insertions of the Z_ψ -counterterms on internal quark propagators always cancel with the $Z_\psi^{\frac{1}{2}}$ -counterterms at the ends of those propagators. Thus, we are left with a *single* power of Z_ψ that corresponds to two external quark lines. The term proportional to $(Z_m - 1)$ is found from

$$[\langle P_k \rangle_{1 \text{ loop}}]_{m_b(\mu) \rightarrow Z_m m_b(\mu)} - \langle P_k \rangle_{1 \text{ loop}}, \tag{6.20}$$

where $\langle P_k \rangle_{1 \text{ loop}}$ is given in eq. (6.6). Remember that $\langle P_7 \rangle_{\text{tree}}$ depends linearly on $m_b(\mu)$.

When all the matrix elements and renormalization constants are substituted into eq. (6.19), one finds that all the $1/\epsilon$ singularities cancel as they should. Furthermore, when the effective Wilson coefficients are used, all the logarithms of m_b/μ are found to be multiplied by numbers from the 7th column of $\hat{\gamma}^{(0)\text{eff}}$ (6.3). Thus, the amplitude M takes the form

$$M = \langle P_7 \rangle_{\text{tree}} \left\{ \left[1 + \frac{\alpha_s}{4\pi} \tilde{r}_7 \right] \left[C_7^{(0)\text{eff}} + \frac{\alpha_s}{4\pi} C_7^{(1)\text{eff}} \right] + \frac{\alpha_s}{4\pi} \sum_{\substack{1 \leq k \leq 8 \\ k \neq 7}} C_k^{(0)\text{eff}} \left[r_k + \gamma_{k7}^{(0)\text{eff}} \ln \frac{m_b}{\mu} \right] \right\}. \tag{6.21}$$

From the above expression, we have read out the results for r_k that have been already given in eq. (3.1).

⁸ Up to an overall normalization factor of $-\frac{4G_F}{\sqrt{2}} V_{ts}^* V_{tb}$.

7 Conclusions

We have computed the two-loop $b \rightarrow s\gamma$ matrix elements of all the four quark operators containing no derivatives. This allowed us to complete the NLO QCD calculation of $\bar{B} \rightarrow X_s\gamma$ decay by including for the first time the two-loop matrix elements of the QCD-penguin operators P_3, \dots, P_6 . The values of the corresponding parameters r_k that enter the branching ratio are collected in table 1. They are also valid in extensions of the SM.

The Wilson coefficients of QCD-penguin operators are small in the SM. Consequently, two-loop matrix elements of these operators affect the $\bar{B} \rightarrow X_s\gamma$ branching ratio by around 1% only. In extensions of the SM, the Wilson coefficients might be larger, which would enhance their phenomenological significance. However, it should be emphasized that the modification of C_i with $i = 3, \dots, 6$ would not only have a NLO effect (via the two-loop contributions evaluated here) but also a LO one (via the effective coefficients in eq. (2.3)).

Since in certain extensions of the SM, new operators with different Dirac and color structures may contribute, we have performed calculations that allow inclusion of such operators if necessary. The relevant results can be found in section 5. However, a complete NLO analysis in the presence of new operators would require extending the 3-loop anomalous dimension computation of ref. [4], which is beyond the scope of the present work.

On the technical side, occurrence of internal b-quark propagators required going beyond the techniques developed in refs. [1, 2] that used expansions in $z = m_c^2/m_b^2$. Our exact calculations valid for any z show that the expansions performed in refs. [1, 2] break down around $z \sim 0.5$, and are very accurate up to $z \sim 0.3$, i.e. well above the physical value of $z \sim 0.1$.

8 Acknowledgements

We are grateful to Paolo Gambino for verifying the influence of our results for r_k on the entries of table 2 and on the final prediction for the branching ratio. J.U. would like to thank Stefan Fritsch and Michael Spranger for fruitful discussions. The work presented here was supported in part by the German Bundesministerium für Bildung und Forschung under the contract 05HT1WOA3 and the DFG Project Bu. 706/1-1, and by the Natural Sciences and Engineering Research Council of Canada. M.M. was supported by the Polish Committee for Scientific Research under grant 2 P03B 121 20.

References

- [1] A. J. Buras, A. Czarnecki, M. Misiak and J. Urban, Nucl. Phys. B **611** (2001) 488 [hep-ph/0105160].
- [2] C. Greub, T. Hurth and D. Wyler, Phys. Rev. D **54** (1996) 3350 [hep-ph/9603404].
- [3] P. Gambino and M. Misiak, Nucl. Phys. B **611** (2001) 338 [hep-ph/0104034].
- [4] K. Chetyrkin, M. Misiak and M. Münz, Phys. Lett. B **400** (1997) 206 [Erratum-ibid. B **425** (1998) 414] [hep-ph/9612313].
- [5] A. J. Buras, M. Misiak, M. Münz and S. Pokorski, Nucl. Phys. B **424** (1994) 374 [hep-ph/9311345].
- [6] P. Gambino and U. Haisch, JHEP **0110** (2001) 020 [hep-ph/0109058].
- [7] K. Chetyrkin, M. Misiak and M. Münz, Nucl. Phys. B **520** (1998) 279 [hep-ph/9711280].
- [8] A.J. Buras, A. Kwiatkowski and N. Pott, Nucl. Phys. **B517** (1998) 353 [hep-ph/9710336];
A. Czarnecki and W.J. Marciano, Phys. Rev. Lett. **81** (1998) 277 [hep-ph/9804252];
C. Bobeth, M. Misiak and J. Urban, Nucl. Phys. **B574** (2000) 291 [hep-ph/9910220].